

# Preliminary Gas Turbine Combustor Design Using a Network Approach

P. J. Stuttaford

P. A. Rubini<sup>1</sup>

School of Mechanical Engineering,  
Cranfield University,  
Cranfield, Bedfordshire, MK43 0AL,  
United Kingdom

*The preliminary design process of a gas turbine combustor often involves the use of cumbersome, geometry restrictive semi-empirical models. The objective of this analysis is the development of a versatile design tool for gas turbine combustors, able to model all conceivable combustor types. A network approach is developed that divides the flow into a number of independent semi-empirical subflows. A pressure-correction methodology solves the continuity equation and a pressure-drop/flowrate relationship. The development of a full conjugate heat transfer model allows the calculation of flame tube heat loss in the presence of cooling films, annulus heat addition, and flame tube feature heat pick-up. A constrained equilibrium calculation, incorporating mixing and recirculation models, simulates combustion processes. Comparison of airflow results to a well-validated combustor design code showed close agreement. The versatility of the network solver is illustrated with comparisons to experimental data from a reverse flow combustor.*

## Introduction

The preliminary design of a combustor involves the application of a large pool of knowledge to **conceptualize** an overall structure, normally requiring the use of cumbersome, geometry restrictive semi-empirical models. The results of such an analysis become the input for more thorough investigations such as **computational** fluid dynamics (CFD) simulations and rig testing. The cost of rig testing and to a lesser degree CFD prohibits their use. Simple empirical models are therefore optimized as much as possible before further advanced development.

Semi-empirical models have the advantage of rapid execution times, on the order of a few minutes or less. This is an advantage for the design engineer as it allows optimization with relatively little time expenditure. The more accurate this initial design process, the more rapid the following phases of design. The limitations of such tools include their restriction to simple geometries; being cumbersome to set up; and having difficulties with convergence when applied to more irregular flow fields. Network methods have the ability to model complicated and unusual geometries effectively and with little numerical difficulty while retaining the advantage of rapid execution.

A network consists of a number of independent subflows linked together to model a physical process. The method has been used with success in modeling large pipe networks (Greyvenstein and Laurie, 1994). Since the orientations of the subflows are independent, multidimensional features such as total-static fed cooling rings may be modeled with ease. Each subflow is defined by a semi-empirical pressure-drop/flow rate relationship and a heat transfer relationship. A pressure correction methodology is used to solve the continuity equation and a pressure-drop/flow rate relationship.

## Gas Turbine Combustor Modeling for Design

Initial gas turbine combustor design procedures are based on overall performance requirements including combustion effi-

ciency, lean **lightoff** and blowoff limits, exit temperature traverse, and emissions of CO and NO<sub>x</sub>.

Mellor and Fritsky (1990) demonstrated the application of a characteristic time model in achieving these goals. The model provided full details of primary and secondary air requirements. Comparisons with rig test data proved reasonably accurate. This form of analysis **provides** a sound basis for more detailed computations, giving predictions of mass flow splits, pressure loss, and heat transfer. The results allow a fine-tuning procedure, improving upon the initial design. Three-dimensional analysis of the **flame** tube enables further optimization before undertaking the costly procedure of rig testing.

Empirically based procedures have led to successful evolutionary combustor improvements, but they exhibit shortfalls when significantly different technological designs from those of proven concepts are **required**. Advances in computational fluid dynamics (CFD) modeling have allowed the successful simulation of gas turbine combustor flows. However, the accuracy of such simulations remains limited by the submodels they employ. CFD computations require the time-consuming procedure of grid generation, boundary condition specification, and obtaining solution convergence.

In **combination**, these two methodologies have proven a valuable combustor design tool (Holdeman et al., 1989). Examples of the successful application of such a procedure to specific combustors are given by Mongia et al. (1986). Historical trend lines and one-dimensional models were used to develop a preliminary design. A three-dimensional **empirical/analytical** procedure was employed to augment the basic design, providing a good qualitative analysis, using the submodels of turbulent reactive flow available. Rizk and Mongia (1991) obtained satisfactory agreement **with** experimental results for a range of combustors under various operating conditions, using a three-dimensional **analytical/empirical** performance model.

The use of three-dimensional computational models is a time-consuming task, and **only** undertaken in an attempt to visualize a combustor for which a preliminary design has already been developed. Phenomena displayed by this more complicated analysis may **lead** to modifications in the design.

A number of empirically based models have been developed in the past. These include turbulent **flame** speed models, where the effect of **turbulence** on the combustion is simulated by calculating a turbulent flame speed based on analogy with laminar

<sup>1</sup> Corresponding author.

Contributed by the International Gas Turbine Institute and presented at the 41st International Gas Turbine and Aeroengine Congress and Exhibition, Birmingham, United Kingdom, June 10-13, 1996. Manuscript received at ASME Headquarters February 1996. Paper No. 96-GT-135. Associate Technical Editor J. N. Shinn.

flame speed; **microvolume burning** models, where mixing and chemical reaction processes are accounted for in a series of turbulent eddies within **small** cubes; stirred reactor models, where each zone is assumed to contain a homogeneous reacting mixture (**Hammond** and **Mellor**, 1970).

**Mellor** (1978) in an evaluation of modular gas turbine models found the approach of **Mosier et al.** (1973), and **Mado** and **Roberts** (1974) the most successful. In this model the internal **flowfield** is approximated by a series of co-annular, one-dimensional **reacting** streamtubes. A one-dimensional streamtube represents the flow recirculation in the primary zone, i.e., a well-stirred reactor. A procedure was developed whereby the streamtubes exchange mass, momentum, and energy via turbulent mixing. The effects of port and film cooling air injection were modeled **semi-empirically**. **Swithenbank et al.** (1973) developed a model containing partially stirred reactors, based on turbulent mixing. The model was shown to predict blow-off stability limits, overall combustion efficiency, combustion intensity, and overall pressure loss. Secondary analysis was **able** to predict emissions and wall heat transfer. The methodology proved useful in analyzing the effects of design modifications.

One-dimensional models, such as that described by **Burus et al.** (1987), have been used successfully for the preliminary design and sizing of a **combustor**. Given target airflow distributions, the required flow areas could be computed, or given the areas, the various flow splits and pressure drops may be calculated. The one-dimensional **models** incorporate numerous experimental data, and empirically derived **correlations** to support the simplified overall **governing** equations (**Mellor**, 1990).

A flexible geometry-independent one-dimensional model, while lacking the resolution of the three-dimensional models, is still able to predict reasonably accurate results very rapidly. The **flexibility** of network analysis allows the simple modeling of complex **geometries**, and removes many of the restrictions placed upon conventional one-dimensional models. The submodels within these **solution** procedures, e.g., equilibrium models, film-cooling models, radiation models, etc., continue to be improved upon. The network approach offers a simple procedure of incorporating the latest submodels in an **algorithm**, enabling the complete modeling of a combustor.

## Numerical Algorithm

The domain of interest is modeled by overlaying a network on the system geometry. The network consists of a number of elements and nodes. The elements represent actual physical features in the domain, e.g., duct sections, holes, etc. The **nodes** join the elements to one another, thus combining independent features into a meaningful overall structure. The overall governing equations are solved within the nodes, while semi-empirical relationships may be employed to describe the flow through an element.

The procedure used for obtaining a solution to the flow equations is the SIMPLE (**Patankar**, 1980) pressure **correction** meth-

odology. The one-dimensional flow may be incompressible or compressible.

The overall governing flow equations are the continuity equation, and a pressure-drop/flow rate relationship (**Greyvenstein** and **Laurie**, 1994). The continuity equation may be specified as,

$$\sum_{j=1}^J \rho_{i,j} Q_{i,j} s_{i,j} = -d_i \quad i = 1, 2, \dots, J \quad (1)$$

and the **pressure-drop/flow-rate** relationship as,

$$\Delta P_{i,j} \equiv P_{n_{i,j}} - P_i \equiv s_{i,j} H_{i,j} g_{i,j} f_{i,j} \quad (2)$$

where

$$g_{i,j} = g_{i,j}(\rho_{i,j})$$

$$f_{i,j} = f_{i,j}(|Q_{i,j}|)$$

$$H_{i,j} = \frac{Q_{i,j}}{|Q_{i,j}|}$$

$$s_{i,j} = 1 \quad \text{if the flow is in the positive direction}$$

$$s_{i,j} = -1 \quad \text{if the flow is in the negative direction.}$$

These functional relationships are derived from semi-empirical formulations for combustor features and internal **flows**. Examples of the formulations, such as the Darcy-Weisbach equation and flow in duct sections, may be found in **Jeppson** (1977) and **Saad** (1985). Internal flow effects such as momentum addition and recirculation could be accounted for in the pressure-drop equations, but only from an empirical standpoint. The functional relationships are written as coefficients in the overall solution matrix, and simultaneously solved using the direct method discussed later in this section.

For an ideal gas,

$$\rho_{i,j} = \frac{P_{i,j}}{RT_{i,j}} \quad \text{or} \quad \rho_{i,j} = \frac{P_i + P_{n_{i,j}}}{2RT_{i,j}} \quad (3)$$

Figure 1 shows a section of a typical network. Initially, the temperatures and pressures at the nodes,  $T_{i,j}^*$  and  $P_{i,j}^*$ , are predicted, and if the flow is compressible Eq. (3). Is used to calculate  $\rho_{i,j}^*$ . Using Eq. (2), a predicted flow-rate,  $Q_{i,j}^*$ , is calculated.

The predictions are corrected using the following relationships:

$$P = P^* + P'$$

$$Q = Q^* + Q'$$

$$\rho = \rho^* + \rho' \quad (4)$$

To correct these values a relationship between the flow rate and pressure is **computed**, obtained by differentiating Eq. (2) with respect to  $Q_{i,j}$ ,

## Nomenclature

$C_p$ = specific heat at constant pressure	$P$ = pressure
$C/H$ = carbon/hydrogen mass ratio of fuel	$Q$ = volumetric flow rate
$d$ = external mass flow into node	$q$ = fuel/air ratio
$E$ = energy source term	$R$ = gas constant
$h$ = convective heat transfer coefficient	$T$ = temperature
$L$ = luminosity	$e$ = convergence parameter
$l_b$ = mean beam length	$\epsilon_g$ = gas emissivity
$m$ = mass flow rate	$\eta$ = <b>film effectiveness</b>
	$\rho$ = density

## Subscripts

$f$ = film
$g$ = hot gas
$i$ = center node
$i, j$ = branch element
$n_{i,j}$ = branch node
$p$ = adjacent upstream location

## Superscripts

*	= predicted values
'	= correction values

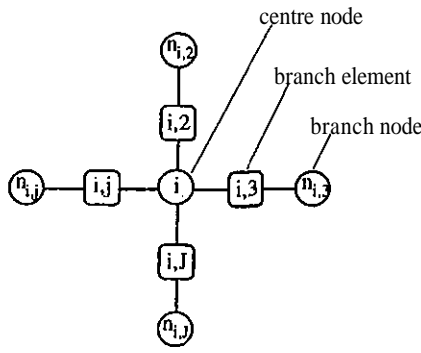


Fig. 1 Network nomenclature

$$Q'_{i,j} = P'_{n_{i,j}} \left[ \frac{1}{s_{i,j} g_{i,j}^* f_{i,j}^* l_{i,j}^*} - \frac{H_{i,j} a_{i,j} f_{i,j}^* g_{i,j}^* l_{i,j}^*}{g_{i,j}^* f_{i,j}^* l_{i,j}^*} \right] - P'_i \left[ \frac{1}{s_{i,j} g_{i,j}^* f_{i,j}^* l_{i,j}^*} + \frac{H_{i,j} a_{i,j} f_{i,j}^* g_{i,j}^* l_{i,j}^*}{g_{i,j}^* f_{i,j}^* l_{i,j}^*} \right] \quad (5)$$

where

$$a_{i,j} = \frac{1}{2RT_{i,j}}; \quad g_{i,j} = \frac{\partial g_{i,j}}{\partial \rho_{i,j}}; \quad f_{i,j} = \frac{\partial f_{i,j}}{\partial |Q_{i,j}|}$$

Substituting Eqs. (4) and (5) into Eq. (1) gives

$$P'_i = \frac{\sum_{j=1}^J (c_{i,j} P'_{n_{i,j}}) + b_i}{c_{i,i}} \quad (6)$$

where

$$c_{i,i} = \sum_{j=1}^J \left[ \frac{\rho_{i,j}^*}{g_{i,j}^* f_{i,j}^* l_{i,j}^*} + s_{i,j} H_{i,j} a_{i,j} \left( \frac{\rho_{i,j}^* f_{i,j}^* g_{i,j}^* l_{i,j}^*}{g_{i,j}^* f_{i,j}^* l_{i,j}^*} - |Q_{i,j}^*| \right) \right]$$

$$c_{i,j} = \frac{\rho_{i,j}^*}{g_{i,j}^* f_{i,j}^* l_{i,j}^*} - s_{i,j} H_{i,j} a_{i,j} \left( \frac{\rho_{i,j}^* f_{i,j}^* g_{i,j}^* l_{i,j}^*}{g_{i,j}^* f_{i,j}^* l_{i,j}^*} - |Q_{i,j}^*| \right)$$

$$b_i = d_i + \sum_{j=1}^J (\rho_{i,j}^* Q_{i,j}^* s_{i,j})$$

Equation (6) is solved simultaneously for all nodes in the network. Updated values for flow rate, pressure, and density are calculated from Eq. (4). The process is repeated until convergence is achieved. The convergence criterion for the continuity equation is,

$$\epsilon_m < \frac{|h_i|_{\max}}{|\dot{m}|_{\text{mean}}} \quad (7)$$

where,

$$h_i = \sum_{j=1}^J (\rho_{i,j} Q_{i,j} s_{i,j}) + d_i$$

and for the pressure-drop equation,

$$\epsilon_p < \sum_{e=1}^E \left| \frac{\Delta P_1 - \Delta P_2}{\Delta P_1} \right| \quad (8)$$

where,

$\Delta P_1$  = pressure drop across element from Eq. (2).

$\Delta P_2$  = pressure difference between two nodes associated with element

The envelope method (George and Liu, 1981) is used to solve Eq. (6) exactly. Formerly, this method is identical to the Gaussian elimination method. Essentially the approach allows significant savings in computing time and storage allocation by not computing quantities known in advance to be zero. A further optimization is made by employing the reverse Cuthill-McKee re-ordering algorithm (George and Liu, 1981). An evaluation of this methodology by Greyvenstein and Laurie (1994) illustrated significant improvements on convergence in comparison to other methods, such as the Newton-Raphson scheme.

The energy equation is satisfied by ensuring an enthalpy balance at each node within the network. This may be specified at nodes with branch elements containing mass transfer as,

$$T_i = \frac{\sum_{j=1}^J (E_{i,j} + \dot{m}_{i,j} C_p T_{n_{i,j}})_{\text{inflow bits}}}{\sum_{j=1}^J (\dot{m}_{i,j} C_p)_{\text{inflow bits}}} \quad (9)$$

where

$$E = H - W$$

= (heat transfer to element) - (work done by element)

A semi-implicit formulation is used to compute node temperatures on boundaries or within walls, i.e., at nodes where the branch elements contain no mass flow. On the flow boundaries, where conduction, convection, and radiation are present, this may be expressed as,

$$T_i = \frac{\left( \sum_{j=1}^J \bar{R}_{i,j} \bar{T}_{n_{i,j}} \right)_{\text{conduction}} + \left( \sum_{j=1}^J \bar{h}_{i,j} \bar{T}_{n_{i,j}} \right)_{\text{convection}} + \dot{Q}_{\text{radiation}}}{\left( \sum_{j=1}^J \bar{R}_{i,j} \right)_{\text{conduction}} + \left( \sum_{j=1}^J \bar{h}_{i,j} \right)_{\text{convection}}} \quad (10)$$

where

$\bar{R}$  = conductive heat transfer coefficient

$\dot{Q}$  = heat flux

and within the solid where conduction is the only mode of heat transfer,

$$T_i = \frac{\left( \sum_{j=1}^J \bar{R}_{i,j} \bar{T}_{n_{i,j}} \right)_{\text{conduction}}}{\left( \sum_{j=1}^J \bar{R}_{i,j} \right)_{\text{conduction}}} \quad (11)$$

The heat transfer coefficient terms in Eq. (10) are evaluated using semi-empirical correlations and data for various cooling types found in gas turbine combustors. The effect of film cooling has a significant effect on the wall temperatures, and must be modeled accurately. The calculations take the form of Nusselt number correlations, employing numerous experimental data. A wide range of cooling effects are modeled, including Z-rings, lipped-rings, slots, effusion patches, and transply patches. Examples of such correlations are given in Lefebvre (1983). Heat pick-up by the fluid moving through the flame tube wall is computed. Multiple films at the same location, originating from different features, are accounted for when computing the effective heat transfer coefficient. The effects of adjacent film temperatures and upstream conditions are incorporated using

$$T_j = T_{fp} (\eta_f / \eta_{fp}) + 0 - \eta_f / \eta_{fp} \left( \frac{T_{fp} - T_g}{2} \right) \quad (12)$$

Radiative fluxes may account for over half the total heat flux "seen" by the flame tube walls. A simple empirical model is presently used to account for radiative heat flux (Lefebvre,

1983). The gas emissivity is calculated using a corrected luminosity for gases containing soot clouds,

$$\epsilon_k = 1 - \exp[-290PL(q_{lh})^{0.5}T_g^{-1.5}] \quad (13)$$

where

$$\text{luminosity, } L = 7.53(C/H - 5.5)^{0.84}$$

The accuracy of such a simple model is limited, since in combustors operating at high pressures, luminous emissivity will be highly dependent upon soot formation and oxidation, not simply on fuel type. A more realistic radiation model is being developed, based upon the discrete transfer methodology of Lockwood and Shah (1981).

The Gauss-Seidel iterative technique with successive over-relaxation is used to solve the node temperatures. The convergence criterion for the energy equation is,

$$\epsilon_e > \sum_{i=1}^N \left| \frac{T_{i,old} - T_{i,new}}{T_{old}} \right| \quad (14)$$

The solution of the flow and energy equations are coupled.

A constrained equilibrium computation (Coupland, 1989) calculates adiabatic flame temperatures from local species concentrations at given fuel/air ratios. The computation is based upon the original chemical equilibrium algorithm developed by Gordon and McBride (1971). During the solution procedure the temperature calculation is performed within specified elements, and the resulting heat release is treated as a source term in the energy equation. The source term from the adiabatic flame temperature calculation is corrected to account for the heat loss within the flame tube.

The equilibrium model constrains certain species concentrations such as CO and CO<sub>2</sub>. The model uses these constraints to compute other species concentrations, and hence flame tem-

perature. The constraints are computed by fitting an efficiency curve to the flame tube centreline. This efficiency curve is a function of overall loading, and is correlated for a number of combustor types, thus making allowance for various injectors and fuel types over a range of operating conditions.

The equilibrium point of a system occurs where a combusting fuel/air mixture decomposes into a mixture of chemical species at a specific temperature. The composition of this equilibrium mixture may be described by a minimization of free energy formulation. Gibbs free energy is given by (Gordon and McBride, 1971),

$$g = \sum_{j=1}^n \mu_j n_j \quad (15)$$

where

$\mu_j$  = chemical potential of species  $j$   
 $n_j$  = concentration of species  $j$

The minimization of free energy is subject to the following constraint;

$$b_i^0 - b_i = 0 \quad i = 1, 2, \dots, l \quad (16)$$

where

$b''$  = assigned number of kilogram - atoms of element  $i$  per kilogram — mole species  $7$

$$b_i = \sum_{j=1}^n a_{ij} n_j \quad i = 1, 2, \dots, l$$

$a_{ij}$  = number of kilogram — atoms of element  $i$  in species  $j$

$l$  = number of elements

$n$  = number of species

Chemical species do not always attain full equilibrium in practical systems. The gas temperature is highly affected, should

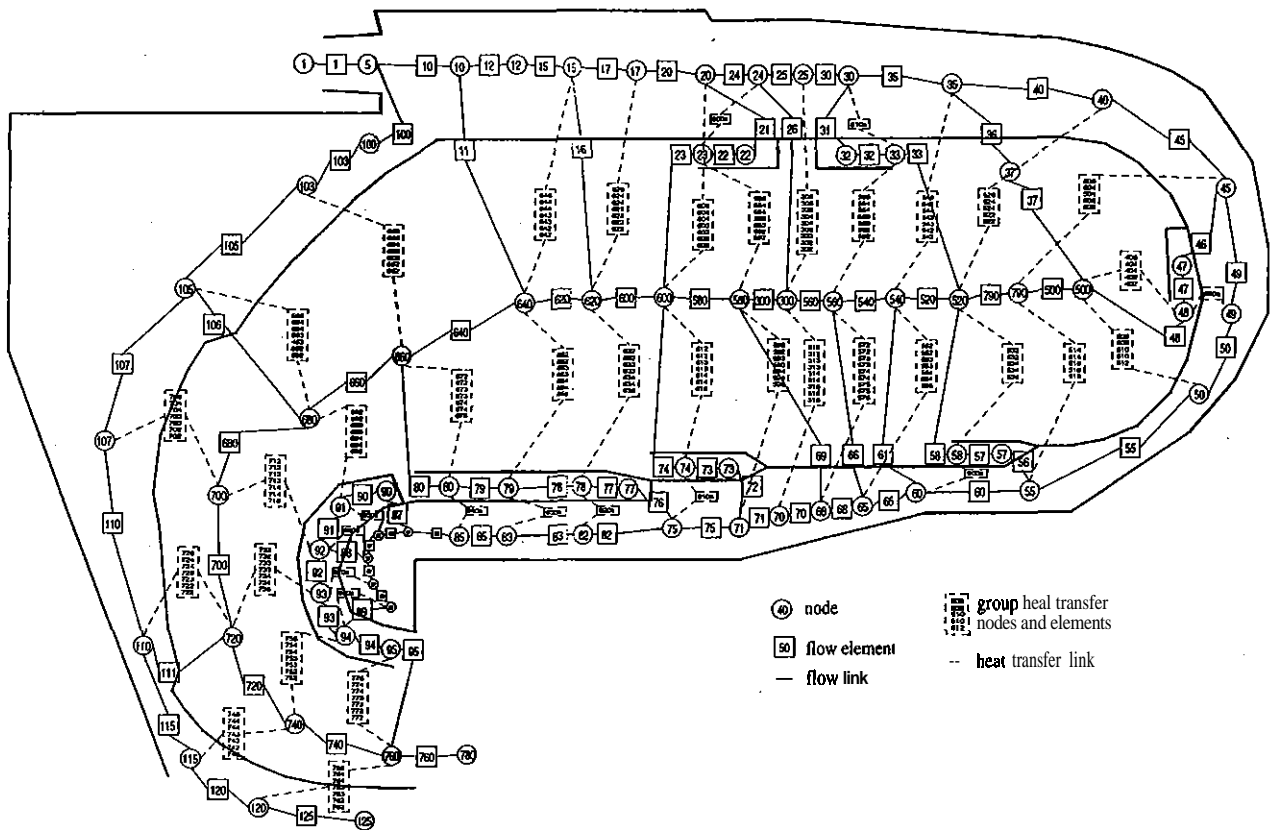


Fig. 2 Network diagram for reverse flow combustor

the fuel/air mixture reach a partial or constrained equilibrium state. This constrained equilibrium may be accounted for by specifying the final concentrations of certain species by setting it as an extra element  $b_i$ , thereby increasing the number of constraints that the calculation is subject to by one per constrained species.

Clearly the most important factor in obtaining a realistic flame temperature is the predicted local fuel/air ratio. A mixing/recirculation model was developed to distribute air from flame-tube ports and cooling features into the combusting flow, based on simple empirically derived rules.

### The Combustor Network

A sample combustor network is shown in Fig. 2. The reverse flow combustor selected for discussion exhibits features that conventional one-dimensional models have difficulty simulating. This includes counterflowing air streams, and extensive double skin features on the liner wall. The dark outline is a not-to-scale representation of the combustor general features. The solid network of elements and nodes refers to the flow computational cells, in which the flow and energy equations are solved. The dashed network represents the heat transfer sequence of elements and nodes required to model the overall heat transfer from the flame tube through the liner to the annuli.

Mass flow splits and pressure drops were computed in the flow logic links, and included various correlations for diffuser, liner hole features, and duct flows. The mixing and recirculation models were used to compute local bulk fuel/air ratios, and this in combination with typical efficiency curves was used to compute local adiabatic flame temperatures from the constrained equilibrium model. The species constrained in this analysis were CO and CO<sub>2</sub>. The heat transfer logic allows for the effects of film cooling, thermal barrier coating, and liner hole heat pick-up. Heat transfer through the double skin regions was also computed.

No restrictions are placed on the network setup. Networks for annular combustors, or combustors with multiple combustion zones, such as double annular combustors, require no additional effort from the user, and the basic methodology for generating the network is identical.

### Results and Discussion

The initial validation of the network solver was undertaken with comparisons to mass flow splits, and pressure drops obtained from a proven industrial one-dimensional combustor code, CODAS (Lowe, 1995), for two annular combustor geometries. The CODAS results generated for these two production combustors have been well validated (Lowe, 1995). The combustors will be simply referred to as Annular Combustor .1 and Annular Combustor .2 for the purposes of this discussion.

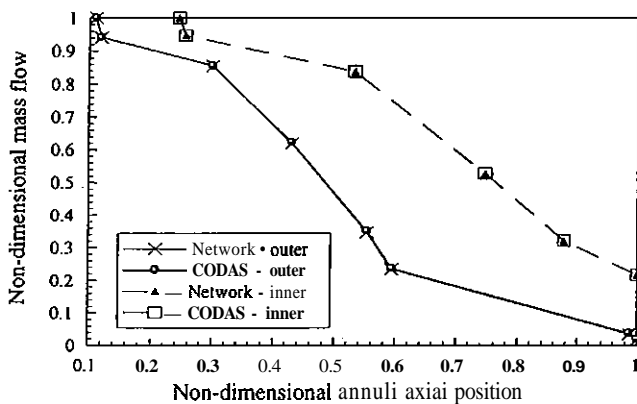


Fig. 3 Annular combustor .1 mass flow split comparison

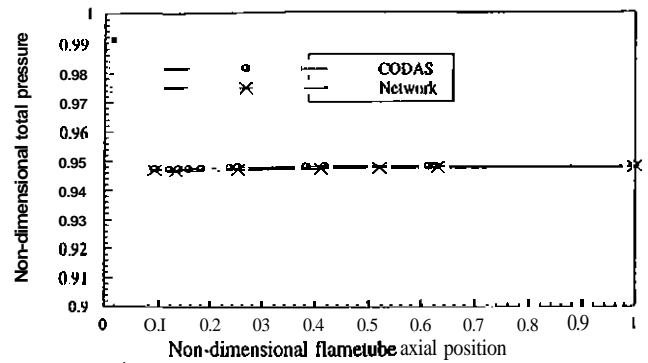


Fig. 4 Annular combustor .1 flame tube total pressure comparison

The mass flow split comparison of Fig. 3 shows the close agreement between CODAS and the network solver. The mass flows are nondimensionalized by the predicted annuli head flows. The liner features through which these flow splits were computed included ports, lipped cooling rings, and effusion patches. Similar methods for the diffuser pressure loss calculation resulted in the close agreement of the head flows. Good agreement was also achieved with the flame tube total pressure profiles shown in Fig. 4. The total pressures include the effects of momentum addition from the liner features. The pressures were nondimensionalized by the combustor total inlet pressure. The difference between the overall pressure loss predicted by the two solvers was within 0.05 percent.

The results for Annular Combustor .2 followed those of the first test case. The results were nondimensionalized as before. Figure 5 shows the close agreement in the annuli mass flow splits. The liner features in this case included ports, lipped rings, total-static-fed slots, static-fed slots, and effusion patches.

The total pressures (see Fig. 6) exhibited close agreement. The baseplate exit pressure differed slightly, resulting in the network solver results being uniformly lower than the CODAS results. The difference was small and resulted from slightly differing treatment of the snout and baseplate region. The pressure rise within the flame tube was in close agreement for the two results. The overall combustor pressure loss differed by 0.2 percent.

The final combustor modeled with the network solver was the reverse flow combustor shown in Fig. 2. The network accounted for momentum addition from the liner features as well as the effects of the radial pressure gradient within the flame tube. The complexity of the reverse flow geometry resulted in only slightly slower convergence than for the annular cases, on the order of a minute on a typical workstation. The airflow

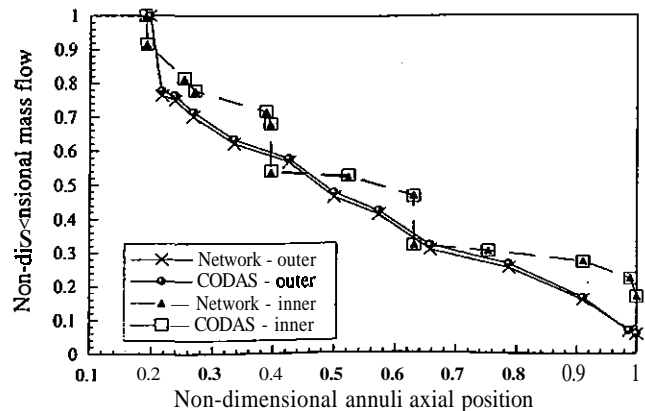


Fig. 5 Annular combustor .2 mass flow split comparison

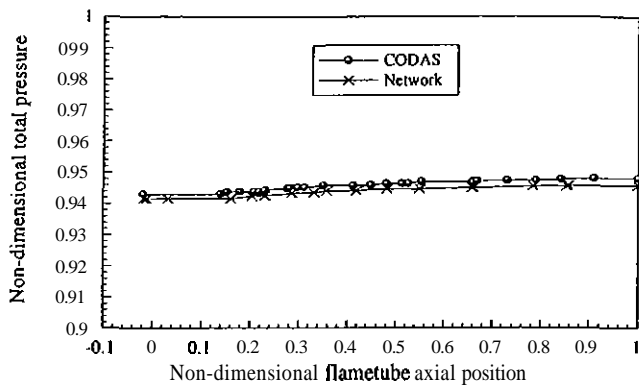


Fig. 6 Annular combustor .2 flame tube total pressure comparison

results for this case could not be compared to CODAS values as in the previous two cases since the CODAS algorithm is unable to model the reverse flow geometry. However, some comparisons were made between the network results and a combination of pressure measurements and corresponding manual calculations (Gardiner, 1995). The overall computed and measured combustor pressure loss agreed within 0.1 percent. Typically, the mass flow splits through the various liner features agreed within approximately 5 percent.

A heat transfer analysis was coupled to the airflow analysis as described in the previous section. The results obtained from this computation were compared to thermal paint data obtained during rig tests (Gardiner, 1995). A sample section of the thermal paint data is presented in Fig. 7. The region below the areas marked "G" corresponds to the diffuser exit plane. The clockwise annulus is in the upward direction. The thermal paint photographs were used to generate the temperature band plots shown in Fig. 8. and Fig. 9.

External wall temperature results generated with the network solver were compared to these temperature bands. The solid line represents the computed values and the shaded region represents the temperature bands of the thermal paint data. Figure 8 shows reasonable agreement between the calculated and measured temperatures. Impingement of combustion gases on the upper liner wall from the primary ports (element "66" in Fig. 2) results in a relatively rapid degradation of the film cooling layer developed by the static ring (elements "22" and "23" in Fig. 2). The dilution ports (element "16" in Fig. 2) within the liner wall resulted in the destruction of any remaining film cooling downstream of the ports. These two effects increased the wall temperature in this region, and appear to be captured by the network solver. The effects of static fed slot film cooling, effusion cooling, and double skins were resolved by the network solver. The accuracy of the computation at the head of the flame tube was limited by the range of validity of the heat transfer correlations.

The thermal paint data extended only as far as element "71" in Fig. 2. The effects of the film cooling would become more

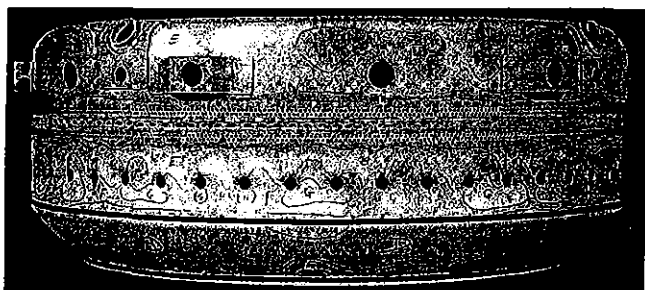


Fig. 7 Sample thermal paint results for reverse flow combustor

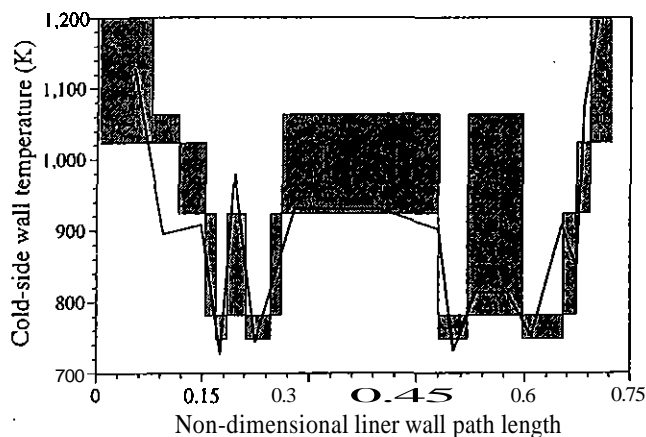


Fig. 8 Clockwise cold-side liner wall temperature comparison

pronounced as the heat transfer network "density" increases. The resolution could be easily manipulated should more detailed information be required. The predicted metal temperatures reached a peak in the final section of the double skinned annulus region, as might be expected since no film cooling is possible in this region. The anticlockwise annulus was cooled by three Z-rings and thermal barrier coated. Figure 9 shows a comparable trend between the computational and experimental results.

The broad bands of the thermal paint data limit the usefulness of the data in assessing the accuracy of the computed results. However, the effects of the various cooling features were captured by the network algorithm.

Predicted wall temperatures varied with flame tube gas temperature, and hence with the recirculation and mixing predicted within the network model. This proved significant in the treatment of the primary port recirculation. The amount of recirculation was simply estimated based on knowledge of the combustor or an understanding of the flowfield generated within the primary zone, from for example CFD predictions.

## Conclusions

A new gas turbine combustor preliminary design methodology has been developed. The network method applied to combustors removes many of the limitations placed upon models by conventional semi-empirical analysis. The network analysis offers versatility as well as computational efficiency for a coupled solution strategy.

Comparisons to a proven airflow analysis code and experimental results have illustrated the ability of the network solver

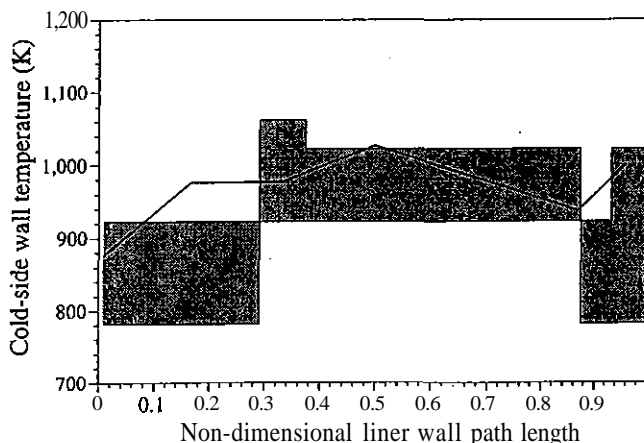


Fig. 9 Anticlockwise cold-side liner wall temperature comparison

to predict mass flow splits and pressure drops accurately within a combustor. Experimental thermal paint results were used to evaluate the heat transfer mechanism within the network code. The nature of the model limited the resolution to assumed circumferential uniformity. The predictive capability of the code was also limited in regions containing significantly varying multidimensional effects. However, the network model was able to predict the trends and ranges of wall temperatures with good qualitative accuracy. Future development of the heat transfer analysis, especially in modeling radiative transfer, is expected to improve the accuracy of the results.

The network approach to gas turbine combustor modeling has been shown to be a versatile and accurate tool in the preliminary gas turbine combustor design procedure.

## Acknowledgments

This work was funded by Rolls-Royce plc and the Defence Research Agency, with technical input from both organizations.

## References

- Burrus, D. L., Shyy, W., and Braaten, M. E. 1987, "Numerical Model for Analytical Predictions of Combustor Aerothermal Performance Characteristics," APGARD CP 422.
- Coupland, J., 1989, Rolls-Royce, U.K., Private Communication.
- Gardiner, J., 1995, Rolls-Royce, U.K., Private Communication.
- George, A., and Liu, J. W., 1981, *Computer Solution of Large Sparse Positive Definite Systems*, Prentice-Hall, Englewood Cliffs.
- Gordon, S., and McBride, B. J., 1971, "Computer Program for Calculation of Complex Chemical Equilibrium Compositions, Rocket Performance, Incident and Reflected Shocks, and Chapman-Jouget Detonations," NASA SP-273, U.S.A.
- Greyvenstein, G. P., and Laurie, D. P., 1994, "A Segregated CFD Approach to Pipe Network Analysis," *International Journal for Numerical Methods in Engineering*, Vol. 37, pp. 3685-3705.
- Hammond, D. C., and Mellor, A. M., 1970, "A Preliminary Investigation of Gas Turbine Combustor Modelling," *Combustion Science and Technology*, Vol. 2, pp. 67-80.
- Holdeman, J. D., Mongia, H. C., and Mularz, E. J., 1989, "Assessment, Development, and Application of Combustor Aerothermal Models," NASA TM-4087.
- Jeppson, R. W., 1977, *Analysis of Flow in Pipe Networks*, Ann Arbor Science, MI.
- Lefebvre, A. H., 1983, *Gas Turbine Combustion*, Hemisphere Publishing Corporation, New York.
- Lockwood, F. C. and Shah, N. G., 1981, "A New Radiation Solution Method for Incorporation in General Combustion Prediction Procedures," *Eighteenth Symposium on Combustion*, The Combustion Institute, Pittsburgh, PA.
- Lowe, D. R., 1995, Rolls-Royce, U.K., Private Communication.
- Mado, R. J., and Roberts, R., 1974, "A Pollutant Emissions Prediction Model for Gas Turbine Combustors," AIAA Paper No. 74-1113.
- Mellor, A. M., 1978, "Turbulent-Combustion Interaction Models for Practical High Intensity Combustors," *Seventeenth Symposium on Combustion*, The Combustion Institute, pp. 377-387.
- Mellor, A. M., and Fritsky, K. J., 1990, "Turbine Combustor Preliminary Design Approach," *Journal of Propulsion and Power*, Vol. 6, No. 3, pp. 334-343.
- Mellor, A. M., ed., 1990, *Design of Modern Turbine Combustors*. Academic Press, New York.
- Mongia, H. C., Reynolds, R. S., and Srinivasan, R., 1986, "Multidimensional Gas Turbine Combustion Modelling: Applications and Limitations," *AIAA Journal*, Vol. 24, No. 6, pp. 890-904.
- Mosier, S. A., Roberts, R., and Henderson, R. E., 1973, "Development and Verification of an Analytical Model for Predicting Emissions From Gas Turbine Combustors during Low-Power Operations," AGARD-CP-125, United Kingdom, pp. 25-1-25-12.
- Patankar, S. V., 1980, *Numerical Heat Transfer and Fluid Flow*, Hemisphere Publishing Corporation, New York.
- Rizk, N. K., and Mongia, H. C., 1991, "Three-Dimensional Analysis of Gas Turbine Combustors," *Journal of Propulsion and Power*, Vol. 7, No. 3, pp. 445-451.
- Saad, M. A., 1985, *Compressible Fluid Flow*, Prentice-Hall, Englewood Cliffs, NJ.
- Swithenbank, J., Poll, I., and Vincent, M. W., 1973, "Combustion Design Fundamentals," *Fourteenth Symposium (International) on Combustion*, The Combustion Institute, Pittsburgh, PA.